

## **Design of an enantioselective artificial metallo-hydratase enzyme containing an unnatural metal-binding amino acid**

Ivana Drienovská<sup>a†</sup>, Lur Alonso-Cotchico<sup>bt</sup>, Pietro Vidossich<sup>b</sup>, Agustí Lledós<sup>b</sup>, Jean-Didier Maréchal<sup>b\*</sup> and Gerard Roelfes<sup>a\*</sup>

\*To whom correspondence should be addressed: j.g.roelfes@rug.nl,

JeanDidier.Marechal@uab.cat

<sup>a</sup>Stratingh Institute for Chemistry, University of Groningen, Nijenborgh 4, 9747 AG Groningen, the Netherlands

<sup>b</sup>Departament de Química, Universitat Autònoma de Barcelona, Edifici C.n., 08193 Cerdanyola del Vallés, Barcelona, Spain

### **Supporting information**

## **Table of contents**

1. Computational studies	S3
2. General experimental and material information	S14
3. Molecular Biology	S14
4. Expression and purification	S17
5. ESI-mass spectra	S18
6. Analytical size exclusion chromatography	S21
7. Catalysis with chiral HPLC traces	S23
8. Saturation Kinetics	S27
9. References	S29

## ***1. Computational studies***

### **Docking**

Protein-ligand docking calculations were performed to assess the complementarity between the cofactor-substrate complex and the protein frame. The crystal structure of the LmrR bound to the drug daunomycin at the dimer interface was used (PDB code: 3F8F)<sup>1</sup>. Crystallographic water molecules and daunomycin were removed from the model. The organometallic complex bipyridine-Cu(II)-substrate was optimized with Gaussian09 program<sup>2</sup> at density functional theory level using B3LYP functional<sup>3,4</sup> and the 6-31g(d,p) basis set<sup>5,6</sup>. A bi-coordinated geometry of the substrate to the copper cofactor was considered, as this is the most suitable to fit the binding site.

For the inclusion of complex at position 89 of LmrR, M89 of each monomer were mutated to alanine using the Dunbrack rotamer library<sup>7</sup> as implemented in UCSF Chimera package<sup>8</sup>. The docking was performed imposing a covalent link between the beta carbon of alanine and the terminal carbon of the bipyridine ligand. Two successive docking runs were performed, the first at position 89 and the resulting structure used for docking at position M89'.

Structures of the LmrR variants M89X\_D100E, M89X\_V15E and M89X\_W96E were generated, first introducing the second mutation using the Dunbrack rotamer library and then performing the docking of the bipyridine-Cu(II) substrate complex as for the wild type protein.

All docking runs were performed with GOLD 5.2 (available through the Cambridge Crystallographic Data Center (CCDC)), and evaluated with ChemScore scoring function<sup>9</sup>.

### **Molecular Dynamics**

The same crystal structure (PDB code: 3F8F) used for the docking was used to set up models for the all-atoms molecular dynamics (MD) simulations. Side chain conformation for residues 71 and 72 of chain A, not determined in the X-ray experiment, were fixed by superposition to chain B. Terminal residues 117-126 of chain A, 1-4 of chain B and 116-126 of chain B, not determined in the X-ray experiment, were discarded and uncharged terminal motifs were used to end the chain terminals. His86, solvent exposed, was considered protonated at e.

Model systems were set up with the xleap program.<sup>10</sup> Each system was embedded into a cubic box including about 37000 water molecules and a number of chloride counterions (4

or 6) as required to neutralize the simulation cell. The AMBER<sup>11</sup> and TIP3P<sup>12</sup> force fields were used for protein and water, respectively. For chloride anions, parameters from ions94.lib library were used.

Parameters for the bipyridine-Cu(II)-substrate complex were developed according to standard approaches. Point charges were calculated with antechamber<sup>10</sup> according to the RESP procedure<sup>13</sup>. Bonded terms at the Cu center were calculated according to Seminario's method based on second-derivatives<sup>14</sup>. The GAFF force field<sup>15</sup> was adopted for the remaining atoms.

A cutoff of 10 Å was used for short range electrostatics and Van der Waals interactions. Long range electrostatic interactions were calculated with the Ewald Particle Mesh method<sup>16</sup>. Bonds involving hydrogen atoms were constrained using the SHAKE algorithm<sup>17</sup>. A time step of 1 fs was used to integrate the equation of motion with a Langevin integrator<sup>18,19</sup>. Constant temperature and pressure were achieved by coupling the systems to a Monte Carlo barostat<sup>20</sup> at 1.01325 bar. Simulations were performed with OpenMM 7.0<sup>21</sup>.

Model systems were initially energy minimized (3000 steps) progressively, allowing water molecules, side-chain and backbone atoms to move; then, thermalization of water molecules and side chains was achieved by increasing the temperature from 100 K up to 300 K; finally, 100 ns MD simulations were performed and further analyzed.

Molecular graphics were performed with the UCSF Chimera package. Chimera is developed by the Resource for Biocomputing, Visualization, and Informatics at the University of California, San Francisco (supported by NIGMS P41-GM103311).

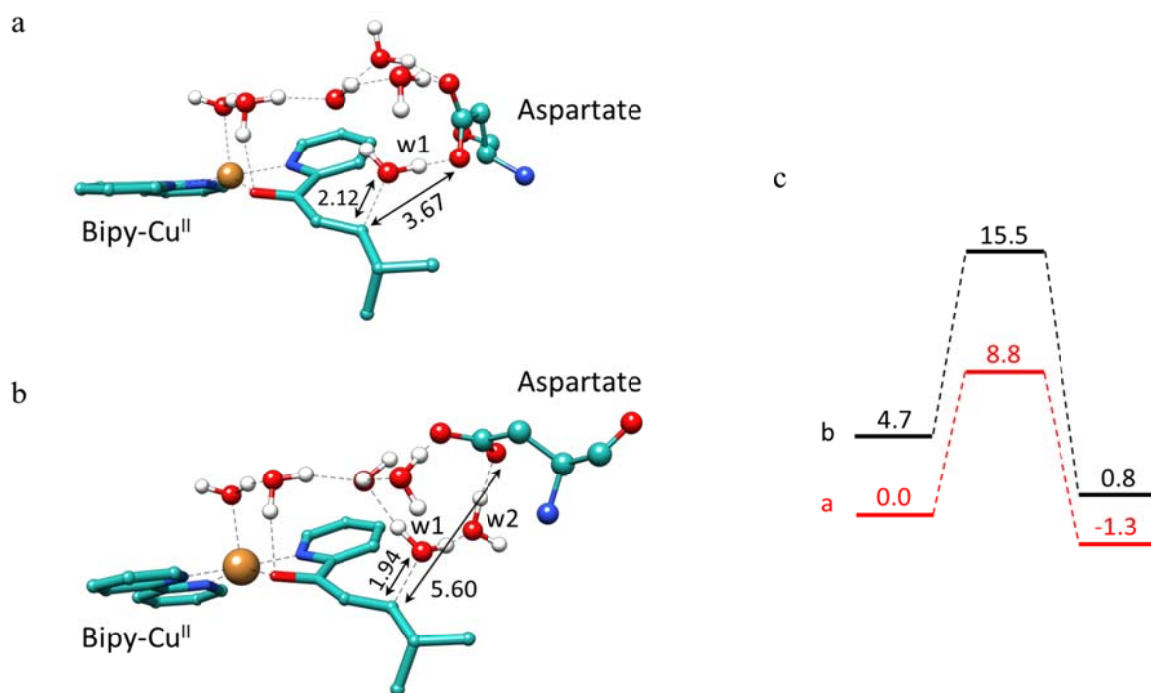


**Figure S1.** Cluster models used to investigate the reaction mechanism of the copper mediated hydration of  $\alpha,\beta$ -unsaturated 2-acyl pyridine. An aspartate amino acid, acting as a base, favors the reaction by activating the nucleophilic water. In a) the nucleophilic water (w1) is directly hydrogen-bonded to the carboxylate. The mechanism for the proton transfer from the nucleophilic water to the carboxylate is also effective via a mediating water molecule (w2), as in b). Shown are the transition states of the reaction, and the  $\Delta G$  values of their respective pathways are represented in c) in kcal/mol.

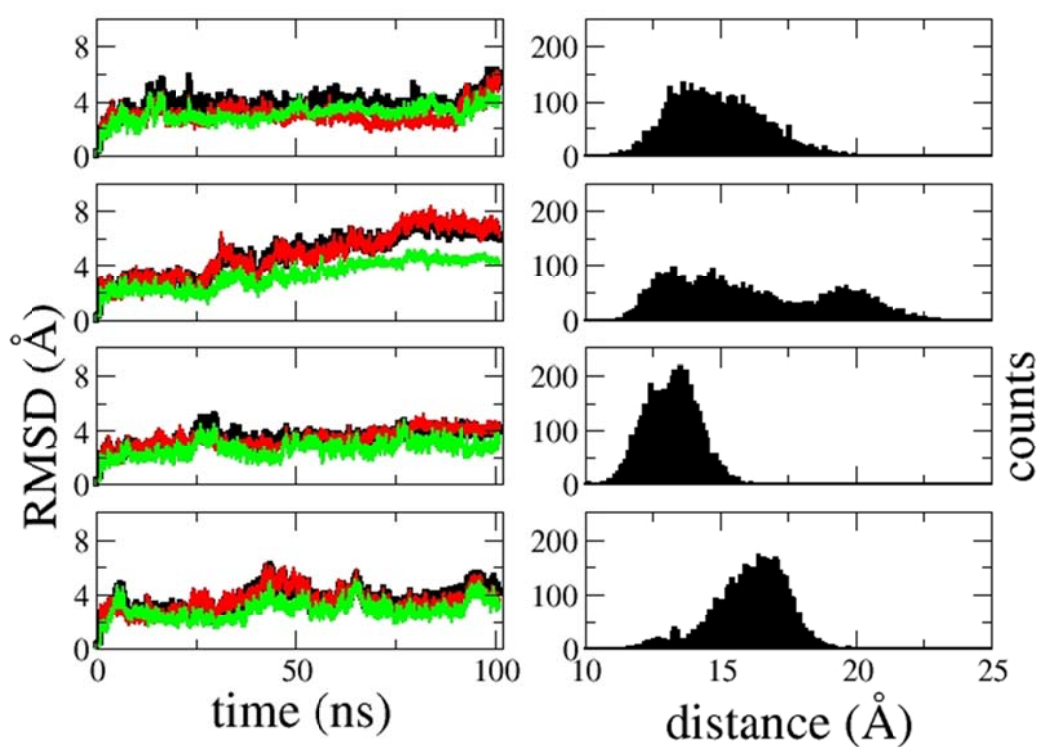


**Figure S2.** Molecular dynamics simulations of (top to bottom) LmrR\_M89X, LmrR\_M89X\_D100E, LmrR\_M89X\_V15E, LmrR\_M89X\_W96E. *Left:* root mean square deviation (RMSD) from the initial structure of the dimer (black line) and each dimer (red and green lines). *Right:* distance between the  $C\alpha$  atoms of residues 96 and 96', which roughly represents the opening of the cavity at the monomer-monomer interface.

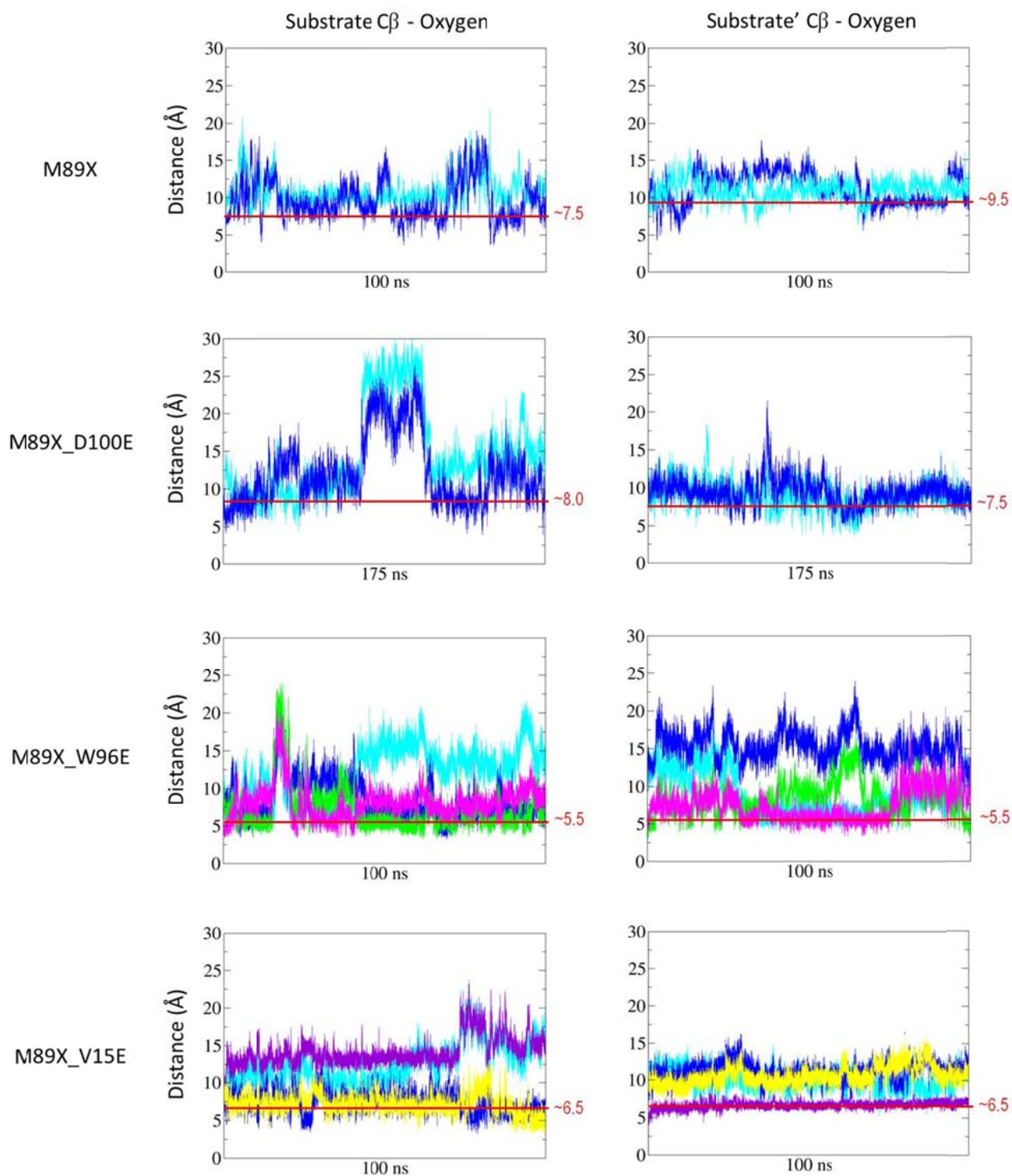


**Figure S3.** Molecular dynamics simulations of LmrR\_M89X, LmrR\_M89X\_D100E, LmrR\_M89X\_V15E, LmrR\_M89X\_W96E. The graphics report the distances between the oxygen atoms of Asp or Glu residues from the electrophilic  $\beta$  carbon of the double bond of the substrate. The coloring: D100/E100 dark blue, D100'/E100' cyan, V15E yellow, V15E' purple, W96E pink, W96E' green.

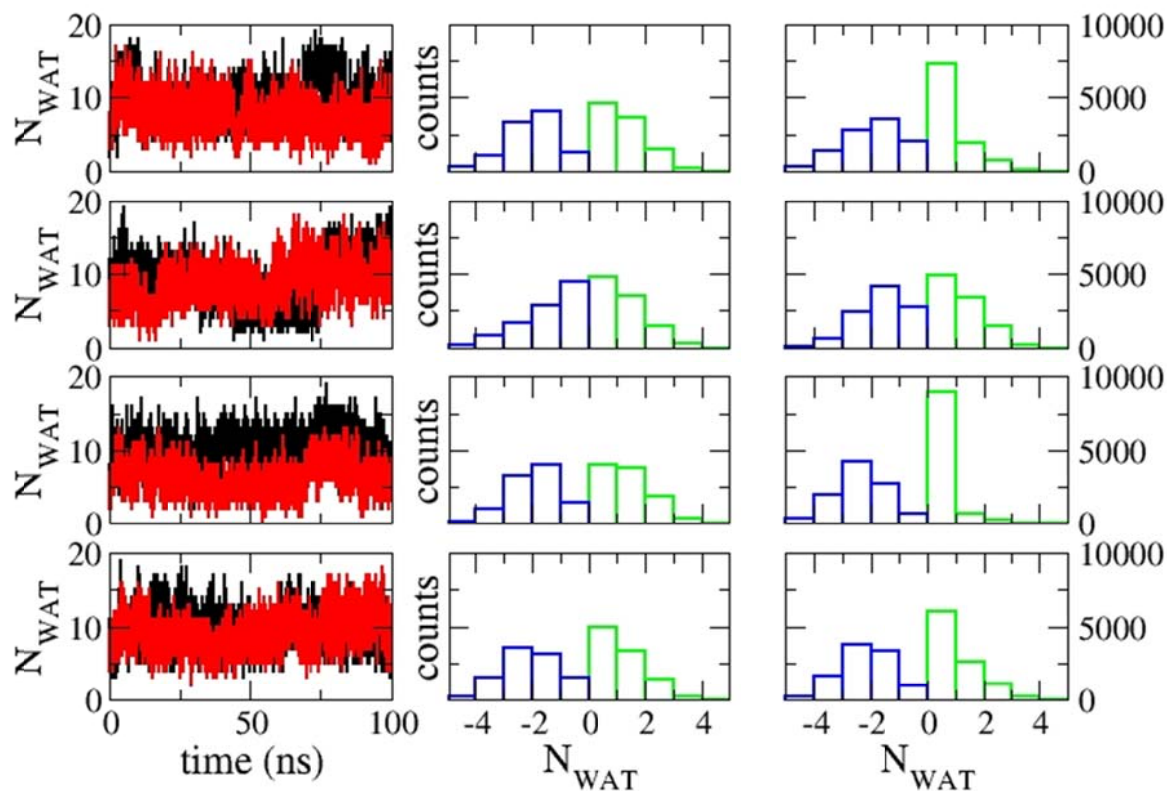


**Figure S4.** Data from the MD simulations of (top to bottom) LmrR\_M89X, LmrR\_M89X\_D100E, LmrR\_M89X\_V15E, LmrR\_M89X\_W96X. *Left column:* time series of the number of water molecules ( $N_{\text{wat}}$ ) within 5 Å from the electrophilic carbon of substrate **1a**. *Middle column:* histogram of  $N_{\text{wat}}$  for BpyA-Cu(II)-**1a**, blue for the pro-S face, green the pro-R face. The histogram tells how many times there are  $N_{\text{wat}}$  waters from the electrophilic carbon of the substrate during the simulation. *Right column:* as the middle column for BpyA- Cu(II)-**1a'**.

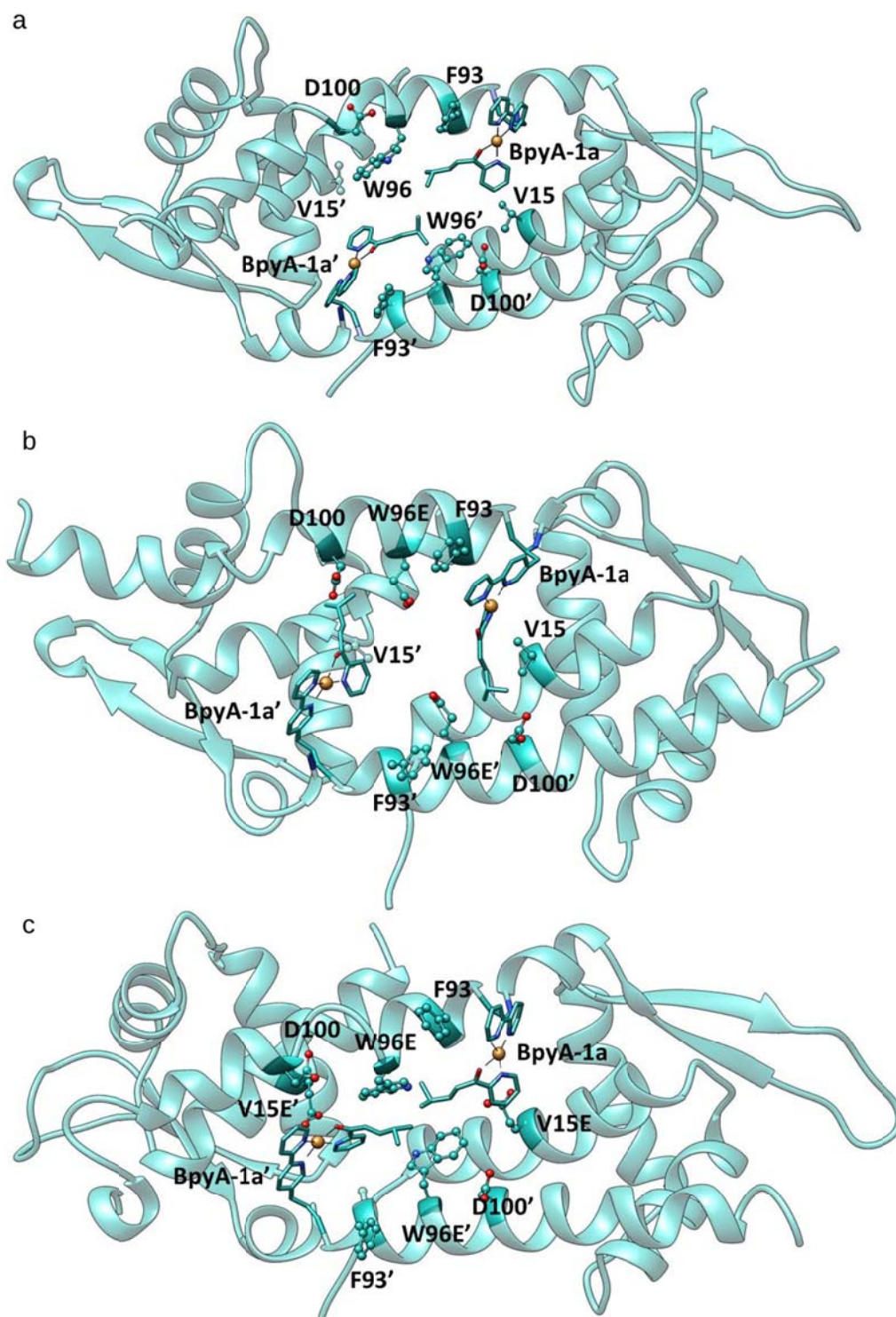


**Figure S5.** Representative structures from the molecular dynamics simulations of a) LmrR\_M89X, b) LmrR\_M89X\_W96E and c) LmrR\_M89X\_V15E.

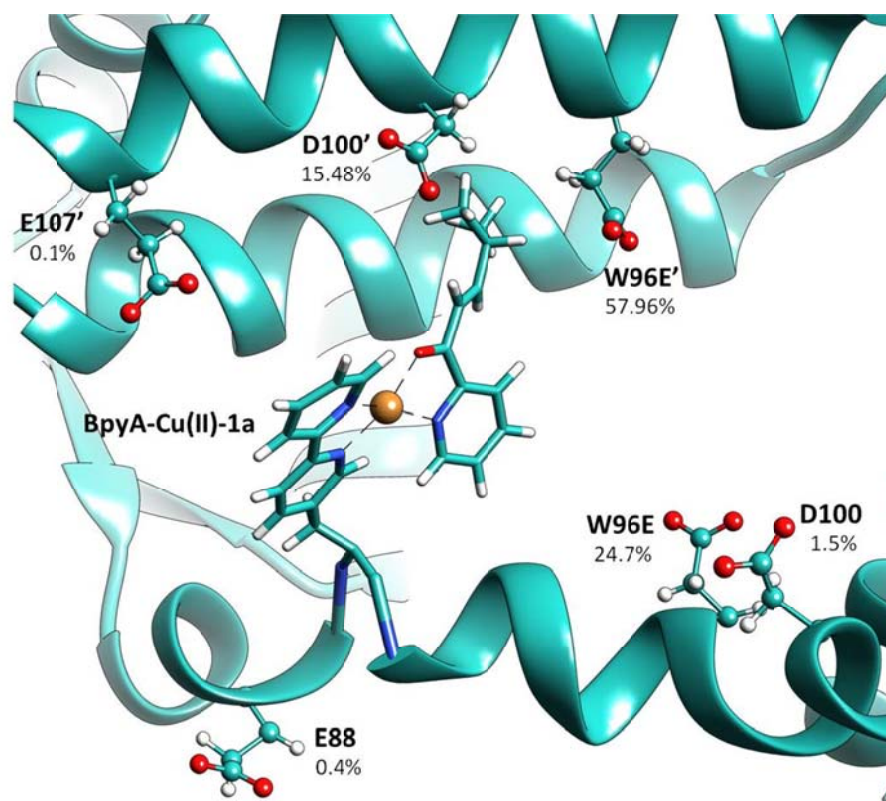


**Figure S6.** Representative structures from the molecular dynamics simulations of LmrR\_M89X\_W96E. The contribution of each specific amino acid to form pre-reactive configurations is indicated.

**Table S1.**

Chemscore predicted values for BpyA-Cu(II)-**1a** docked at one or two monomers of the systems under study.

System	Mon'	Mon	Score	DG	S(hbond)	S(metal)	S(lipo)	H(rot)	DE(clash)	DE(int)	DE(cov)	intocor	S(protein)
LmrR_M89X	BpyA-Cu(II)-1a'	--	47.39	-30.18	0.00	0.00	233.01	1.00	-18.83	0.15	0.26	0.00	1.21
		BpyA-Cu(II)-1a	42.07	-27.69	0.00	0.00	211.67	1.00	-17.22	0.04	1.57	0.00	1.23
LmrR_M89X_V15E	BpyA-Cu(II)-1a'	--	44.40	-30.23	0.00	0.00	233.38	1.00	-17.96	0.21	0.41	0.00	3.16
		BpyA-Cu(II)-1a	41.01	-27.03	0.00	0.00	206.05	1.00	-16.17	0.03	0.91	0.00	1.24
LmrR_M89X_W96E	BpyA-Cu(II)-1a'	--	40.00	-22.76	0.00	0.00	169.54	1.00	-18.73	0.03	0.26	0.00	1.20
		BpyA-Cu(II)-1a	39.48	-23.20	0.00	0.00	173.30	1.00	-18.95	0.00	1.44	0.00	1.22
LmrR_M89X_D100E	BpyA-Cu(II)-1a'	--	47.58	-30.38	0.00	0.00	234.71	1.00	-18.83	0.17	0.26	0.00	1.20
		BpyA-Cu(II)-1a	42.36	-27.93	0.00	0.00	213.73	1.00	-17.26	0.04	1.58	0.00	1.21
LmrR_M89X_M8E	BpyA-Cu(II)-1a'	--	46.99	-30.81	0.00	0.00	238.37	1.00	-19.02	0.02	1.57	0.00	1.25
		BpyA-Cu(II)-1a	41.53	-29.18	0.00	0.00	224.45	1.00	-15.48	0.35	1.02	0.00	1.77
LmrR_M89X_A92E	BpyA-Cu(II)-1a'	--	40.74	-26.88	0.00	0.00	204.77	1.00	-17.84	0.00	0.85	0.00	3.12
		BpyA-Cu(II)-1a	41.87	-33.38	0.00	0.00	260.33	1.00	-12.93	0.02	1.86	0.00	2.55
LmrR_M89X_S95E	BpyA-Cu(II)-1a'	--	47.35	-30.16	0.00	0.00	232.84	1.00	-18.83	0.17	0.26	0.00	1.20
		BpyA-Cu(II)-1a	42.02	-27.59	0.00	0.00	210.90	1.00	-17.28	0.03	1.61	0.00	1.22
LmrR_M89X_Q12E	BpyA-Cu(II)-1a'	--	45.28	-30.14	0.00	0.00	232.67	1.00	-16.84	0.03	0.47	0.00	1.20
		BpyA-Cu(II)-1a	40.85	-31.91	0.00	0.00	247.82	1.00	-12.53	0.02	2.35	0.00	1.23

**Table S2.** Docking predicted distances between the mutated residues and the double bond (C $\alpha$ ) of both substrates.

System	Residue	BpyA-Cu(II)-1a-C $\alpha$	BpyA-Cu(II)-1a'-C $\alpha$
LmrR_M89X	D100	5.72	6.04
	D100'	6.22	8.62
LmrR_M89X_V15E	V15E	3.76	6.85
	V15E'	7.34	3.74
LmrR_M89X_W96E	W96E	3.23	5.42
	W96E'	3.91	5.45
LmrR_M89X_D100E	D100E	5.51	6.51
	D100E'	7.62	9.87
LmrR_M89X_M8E	M8E	8.75	3.95
	M8E'	8.67	10.21
LmrR_M89X_A92E	A92E	15.42	16.92
	A92E'	17.66	13.63
LmrR_M89X_S95E	S95E	9.79	13.73
	S95E'	13.18	12.21
LmrR_M89X_Q12E	Q12E	8.34	7.12
	Q12E'	7.57	8.26

**Table S3.** Data from MD simulations. For each variant, the table reports the number of times a pre-reactive conformation involving a given Asp or Glu residue is observed. 10,000 frames from 100 ns MD simulations were analyzed.

variant	BpyA-Cu(II)-1a		BpyA-Cu(II)-1a'	
	Pro-R face	Pro-S face	Pro-R face	Pro-S face
<b>M89X</b>	D100' – 866 E104' – 1 E107' – 6	E94 – 34 D100' – 7 E104' – 1	D100 – 100 E104 – 9 E107 – 14	--
<b>M89X_D100E</b>	E100 – 45 E100' – 257 E104' – 16 E107' – 193	E87 – 45 E100 – 5 E100' – 30	E100 – 366 E104 – 13 E100' – 13	E100 – 34 E94' – 1 E100' – 1
<b>M89X_V15E</b>	E15 – 904 D100' – 1235 E107' – 2	E15 – 503 D101 – 1 D100' – 215	E15' - 263	D100 – 4
<b>M89X_W96E</b>	E96 – 384 D100 – 19 E96' – 293 D100' – 793 E107' – 3	E87 – 19 E96 – 908 D100 – 58 E96' - 2744 D100' – 18	E7 – 32 E96 – 314 D100 – 80 E104 – 64 E107 – 13 E97' – 32	E7 – 3 E96 – 1650 D100 – 384 E104 – 4 E97' – 1238

**Table S4.** Number of pro-reactive conformations with a distance between the C $\beta$  of the substrate and the O@D/E less than 5 Å. 10,000 frames from 100 ns MD simulations were analyzed.

variant	BpyA-Cu(II)-1a		BpyA-Cu(II)-1a'	
	Pro-R face	Pro-S face	Pro-R face	Pro-S face
<b>M89X</b>	113	1	123	0
<b>M89X_D100E</b>	44	12	51	5
<b>M89X_V15E</b>	541	217	97	0
<b>M89X_W96E</b>	739	1528	172	1300

## **2. General experimental and material information**

*E. coli* strains NEB5-alpha and BL21(DE3) (*New England Biolabs*) were used for cloning and expression. DNA sequencing was carried out by *GATC-Biotech* (Berlin, Germany). Primers were synthesized by *Eurofins MWG Operon* (Ebersberg, Germany). Restriction endonucleases were purchased from *New England Biolabs*. Plasmid Purification Kit was purchased from *QIAGEN*. *Pfu* Turbo polymerase was purchased from *Agilent*. Strep-tactin columns were purchased from *Iba-lifesciences*. Chemicals were purchased from Sigma Aldrich and used without further purification. Concentrations of DNA and protein solutions were estimated based on the absorption at 260 nm or 280 nm on Thermo Scientific Nanodrop 2000 UV-Vis spectrophotometer.

## **3. Molecular biology**

### ***Site-directed mutagenesis***

Site-directed mutagenesis was used for preparation of all LmrR mutants. It was performed on the previously reported plasmid (according to the needed mutation), pET17b\_LmrR\_LM\_M89X<sup>22</sup> (LM–referred to lysine mutants exchanged to K55D, K59Q; M89X – TAG codon at positions 89). The primers required for the mutagenesis are summarized in the Table S5. The following PCR cycles were used: initial denaturation at 95 °C for 1 min, denaturation at 98 °C for 30 s, annealing at 54-63 °C for 30 s (depending on the  $T_m$  of the particular mutant) and extension at 72 °C for 4 min 30 s. The thermal cycle was repeated 16 times and final extension at 72 °C for 10 min was used. The resulting PCR product was digested with restriction endonuclease *DpnI* for 2h at 37 °C and transformed into the chemically competent *E. coli* NEB5-alpha cells. A single colony was cultured in 5 ml of LB medium, the plasmid was isolated and successful mutagenesis was confirmed by sequencing.

**Table S5.** Primers used for site-directed mutagenesis

Primer*	Sequence 5' → 3'
LmrR_M89X_ <b>V15E</b> _fw	GCT CAA ACC AAT GAA ATC CTG CTG AAT
LmrR_M89X_ <b>V15E</b> _rv	ATT CAG CAG GAT TTC ATT GGT TTG AGC
LmrR_M89X_ <b>V15Q</b> _fw	GCT CAA ACC AAT CAG ATC CTG CTG AAT
LmrR_M89X_ <b>V15Q</b> _rv	ATT CAG CAG GAT CTG ATT GGT TTG AGC
LmrR_M89X_ <b>W96E</b> _fw	GCG TTC GAA TCC GAA AGT CGT GTG GAC
LmrR_M89X_ <b>W96E</b> _rv	GTC CAC ACG ACT TTC GGA TTC GAA CGC
LmrR_M89X_ <b>W96Q</b> _fw	GCG TTC GAA TCC CAG AGT CGT GTG GAC
LmrR_M89X_ <b>W96Q</b> _rv	GTC CAC ACG ACT CTG GGA TTC GAA CGC
LmrR_M89X_ <b>D100E</b> _fw	TGG AGT CGT GTG GAA AAA ATC ATT GAA
LmrR_M89X_ <b>D100E</b> _rv	TTC AAT GAT TTT TTC CAC ACG ACT CCA
LmrR_M89X_ <b>D100Q</b> _fw	TGG AGT CGT GTG CAG AAA ATC ATT GAA
LmrR_M89X_ <b>D100Q</b> _rv	TTC AAT GAT TTT CTG CAC ACG ACT CCA

\*In red bold mutation which was introduced by the particular primers set.

#### ***4. Expression and purification***

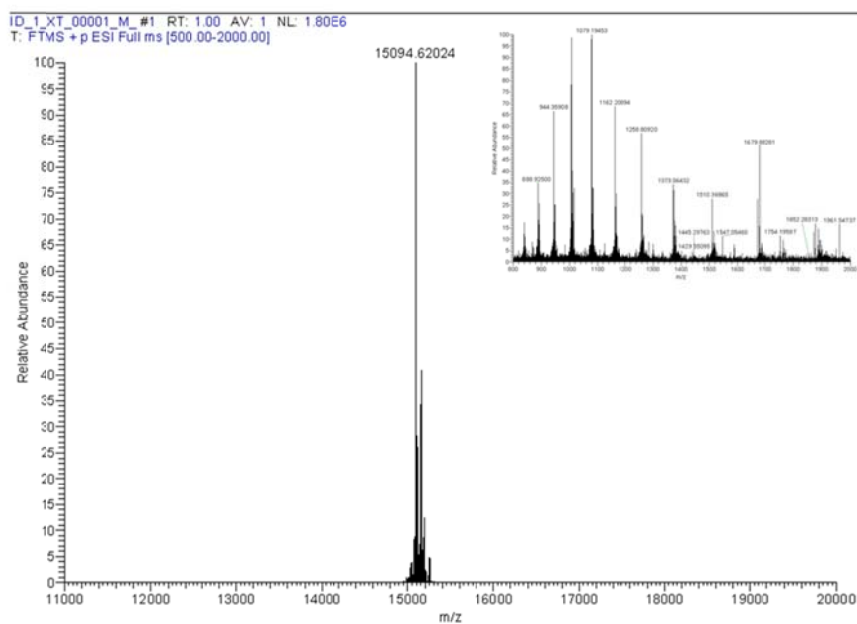
The plasmids pEVOL-BpyAla<sup>23</sup> and pET17b\_LmrR\_X were cotransformed into *E. coli* BL21(DE3) and a single colony was used to inoculate an overnight culture of 10 mL of fresh LB medium containing 100 µg/mL of ampicillin and 34 µg/ml of chloramphenicol at 37 °C. 2 mL (500x dilutions) of overnight culture was used to inoculate at 37 °C 500 mL of fresh LB medium containing 100 µg/mL of ampicillin 34 µg/ml of chloramphenicol. When the culture reached an optical density at 600 nm of 0.8–0.9, the expression was induced with isopropyl β-D-1-thiogalactopyranoside (IPTG) (final concentration 1 mM) and L-Arabinose (final concentration 0.02%) and 200 mg/L of BpyAla (racemic mixture, synthesis previously reported<sup>22</sup>) was added. Expression was done overnight at 30 °C. Cells were harvested by centrifugation (6000 rpm, JA10, 20 min, 4 °C, Beckman), resuspended in washing buffer (50 mM NaH<sub>2</sub>PO<sub>4</sub>, 150 mM NaCl, 50 mM EDTA pH 8.0) and sonicated (70% (200W) for 7 min, 10 sec on, 15 sec off). After centrifugation (15000 rpm, JA-17, 1h, 4 °C, Beckman), the supernatant was loaded on a Strep-Tactin column (Strep-Tactin<sup>®</sup>Superflow<sup>®</sup> high capacity) and incubated for 1 h at 4°C. The column was washed with 3 x 1 CV washing buffer, and eluted with 6 x 0.5 CV of resuspension buffer (same as washing buffer plus 5 mM desthiobiotin). The fractions were analysed by SDS-PAGE electrophoresis on 12% polyacrylamide SDS-TrisTricine gel followed by Coomassie staining (InstantBlue<sup>™</sup>, *Expedeon*). The concentration of the proteins was determined by using the calculated extinction coefficient for LmrR corrected for the absorbance of the BpyAla. Expression yields were 8-15 mg/L. For the purposes of characterization and catalysis, protein solutions were dialyzed against MOPS buffer (20 mM MOPS, 250 mM NaCl, pH 7.0) overnight at 4 °C with 2 exchanges of buffer. Expression in minimal media was also performed for the mutant LmrR\_M89X\_V15E and LmrR\_M89X\_W96E to minimize the iron binding. Protocol as mentioned above was followed, with only exception, that is expression at 30 °C for two days, instead of one.

## 5. Exact mass spectra

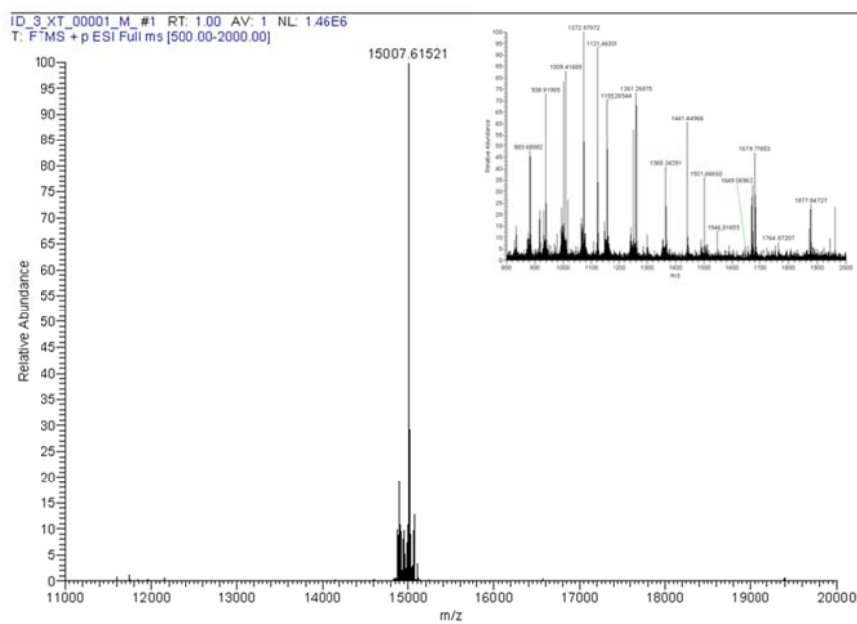
Exact mass of the proteins was recorded on an Orbitrap XL (Thermo Scientific, ESI positive mode).

**Figure S7.** Mass spectra of the different LmrR mutants.

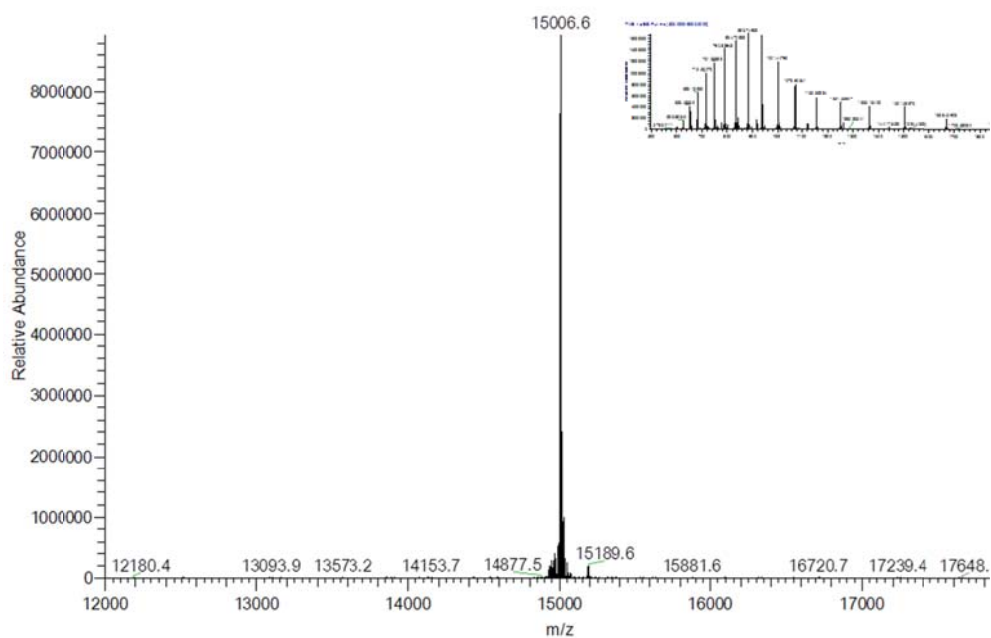
**LmrR\_M89X\_V15E** calculated mass (-Met) 15094.59



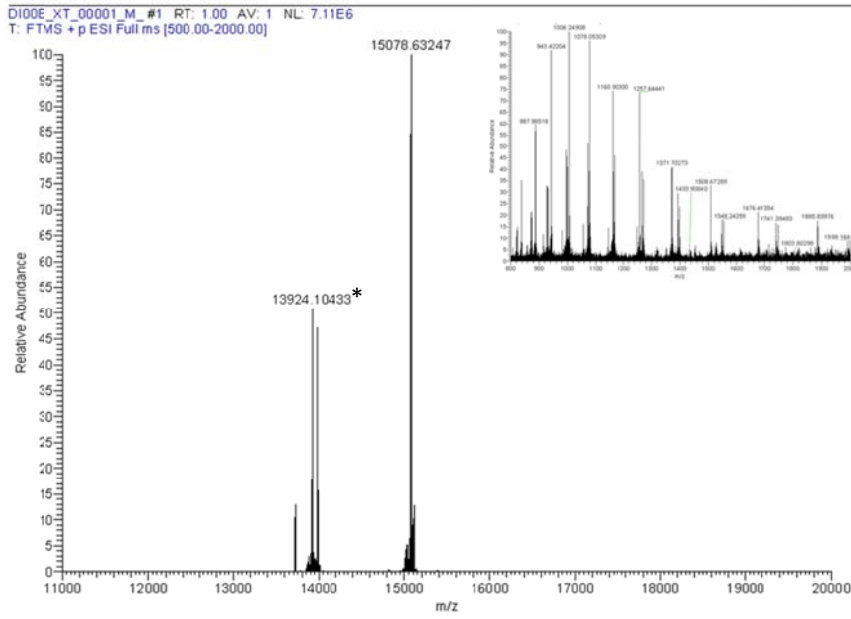
LmrR\_M89X\_W96E calculated mass (-Met) 15007.51



LmrR\_M89X\_W96Q calculated mass (-Met) 15006.53

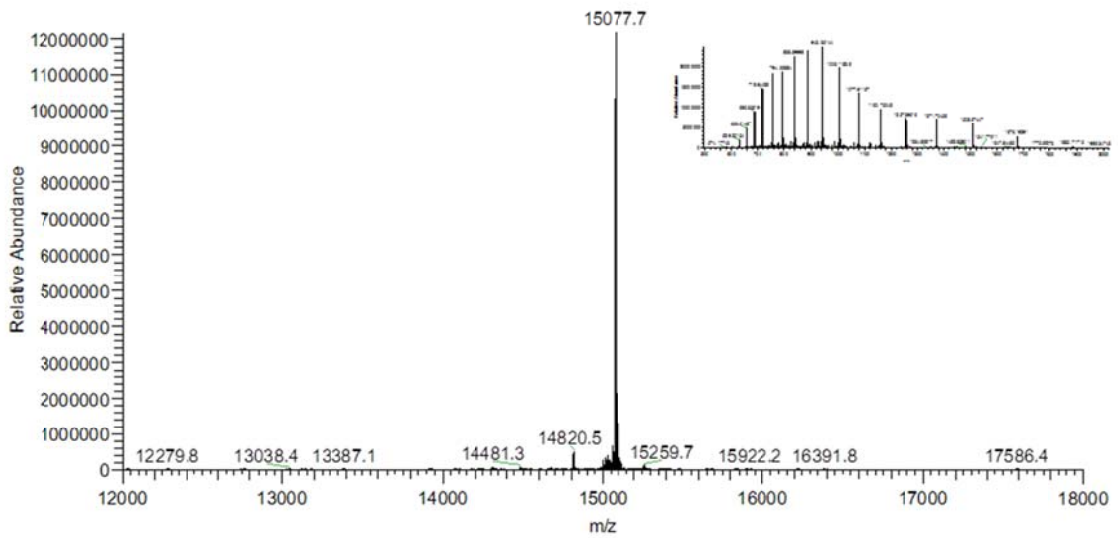


LmrR\_M89X\_D100E calculated mass (-Met) 15078.64



\*13924.1 - degradation/cut of the protein - without terminal 10 amino acids (GG + Streptag)

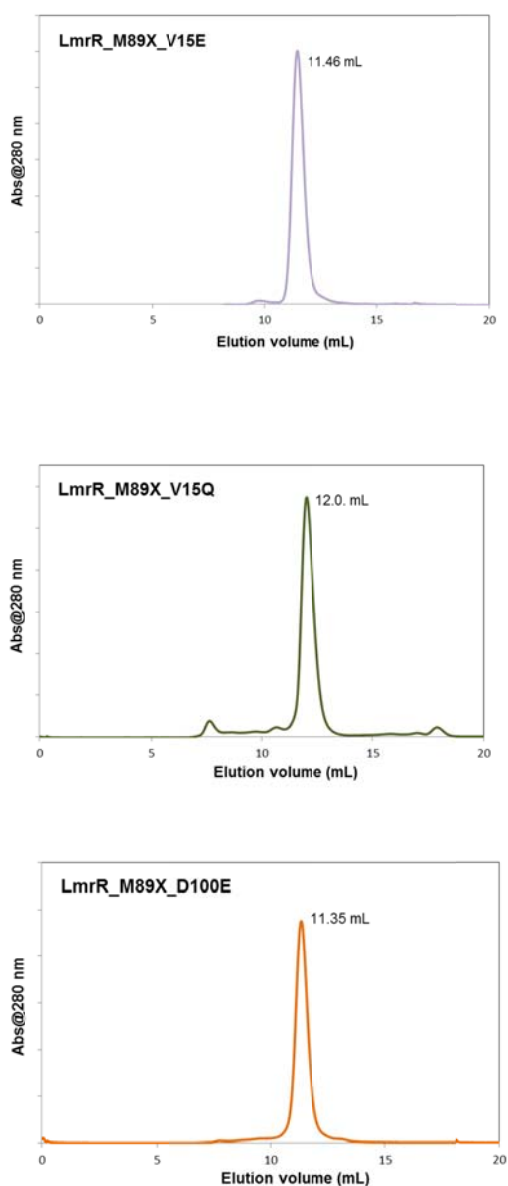
LmrR\_M89X\_D100Q calculated mass (-Met) 15077.66

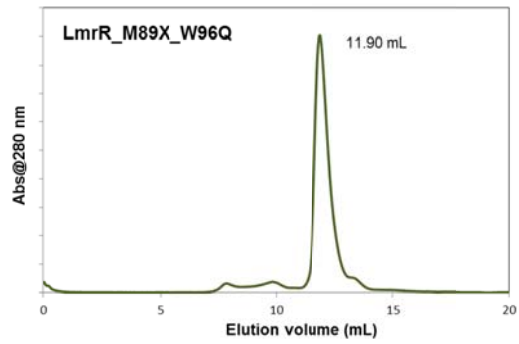
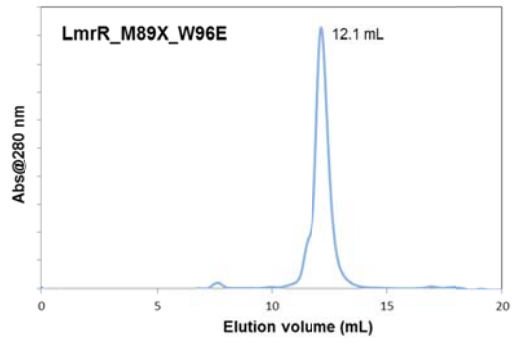
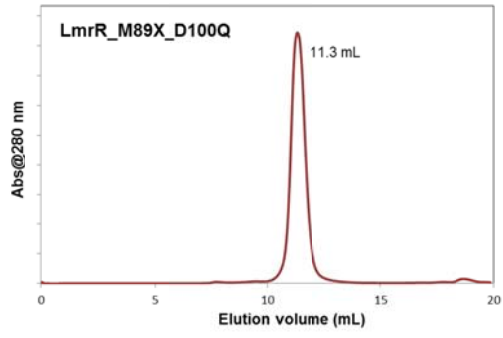


## 6. Analytical size-exclusion chromatography

Analytical size-exclusion chromatography was carried out using the Superdex-75 10/300 GL size-exclusion column (*GE Healthcare*). 100  $\mu$ l of the sample was injected, using MOPS (20 MOPS, 250 mM NaCl, pH 7.0) as a buffer (flow 0.5 ml/min). The column was calibrated using the standard Gel Filtration LMW Calibration Kit (*GE Healthcare*). The results show LmrR mutants all eluting as single peak at the elution volume of 11.6 ( $\pm$  0.4) ml, which is consistent with the homodimeric structures of molecular weight around 30 kDa (Figure S8).

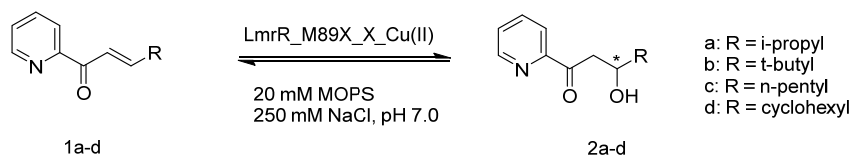
**Figure S8.** Analytical size exclusion chromatography (Superdex-75 10/300 GL) of prepared LmrR mutants.





## 7. Catalysis

*Representative procedure for water-addition reaction catalyzed by LmrR\_M89X\_X\_Cu(II).*



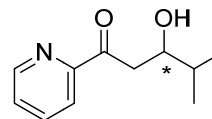
The catalytic solution was prepared by combining  $\text{Cu}(\text{H}_2\text{O})_6(\text{NO}_3)_2$  (90  $\mu\text{M}$ , 9 % catalyst loading) with 1.25 equivalents of LmrR\_M89X\_X (112.5  $\mu\text{M}$ ) in a final volume of 290  $\mu\text{L}$  MOPS buffer (20 mM MOPS, 250 mM NaCl, pH 7.0) and incubating together at 4  $^\circ\text{C}$  for one hour. To this 10  $\mu\text{L}$  of a fresh stock solution of substrate **1** in  $\text{CH}_3\text{CN}/\text{MOPS}$  (50:50, 30mM, final concentration in reaction mixture 1 mM). The reaction was mixed for 3 days by continuous inversion at 4  $^\circ\text{C}$ . The product was extracted with 3 x 1 mL of diethyl ether, the organic layers were dried on  $\text{Na}_2\text{SO}_4$ , and evaporated under reduced pressure. The product was redissolved in 200  $\mu\text{l}$  of a heptane:propan-2-ol mixture (10:1) and the conversion and enantiomeric excess were determined using np-HPLC. Substrates and products of tested reactions have been synthesized according to previously published procedures.<sup>24</sup>

Chiral HPLC traces

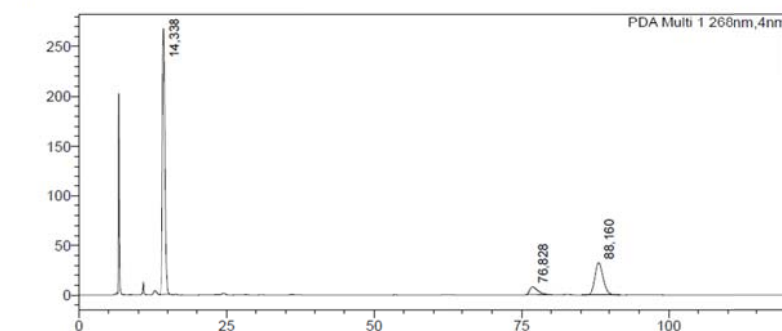
**Figure S9** Chiral HPLC traces of products of the water-addition reaction catalyzed by LmrR\_M89X\_X-Cu(II)

**2a** (Chiralpak-ADH n heptane:iPrOH 99:1, 0.5 ml/min)

SHIMADZU LabSolutions **2a**



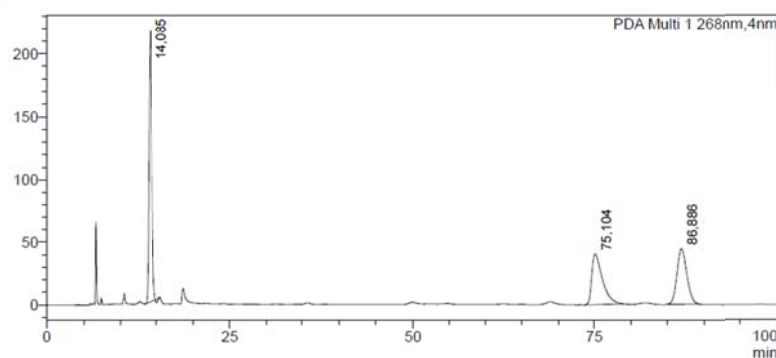
<Chromatogram>  
mAU



Peak#	Ret. Time	Area	Height	Conc.	Unit	Mark	Name
1	14.338	8427779	266676	0.000		M	
2	76.828	723213	7788	0.000		M	
3	88.160	3170822	32542	0.000		M	
Total		12321814	307007				

SHIMADZU LabSolutions **2a racemate**

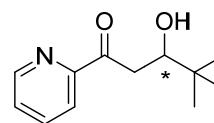
<Chromatogram>  
mAU



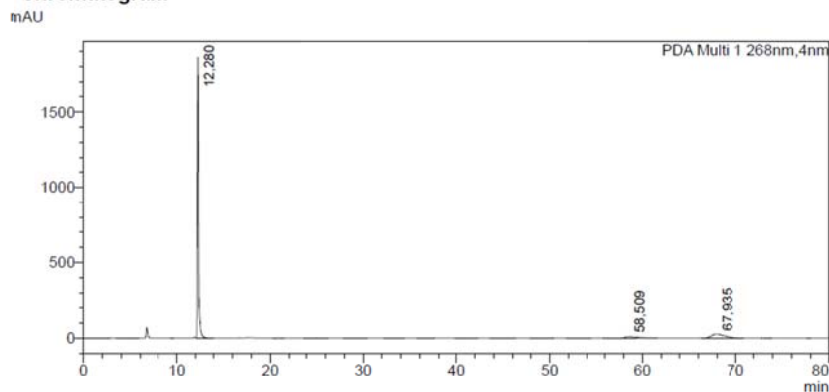
Peak#	Ret. Time	Area	Height	Conc.	Unit	Mark	Name
1	14.085	6156846	216355	0.000		M	
2	75.104	4058108	40232	0.000		M	
3	86.886	4117749	44177	0.000		M	
Total		14332703	300764				

**2b** (Chiralpak-ADH n heptane:iPrOH 99:1, 0.5 ml/min)

SHIMADZU LabSolutions **2b**



<Chromatogram>

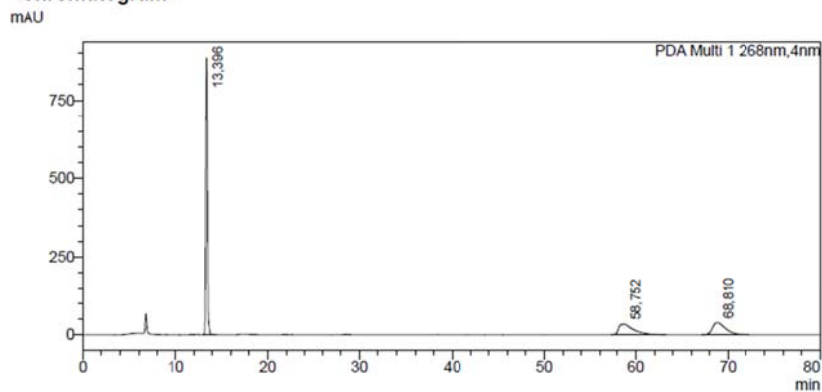


<Peak Table>

Peak#	Ret. Time	Area	Height	Conc.	Unit	Mark	Name
1	12.280	16080736	1862515	0,000		V	
2	58.509	856636	9743	0,000		S	
3	67.935	2544124	25807	0,000			
Total		19481496	1898066				

SHIMADZU LabSolutions **2b racemate**

<Chromatogram>

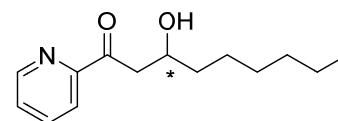


<Peak Table>

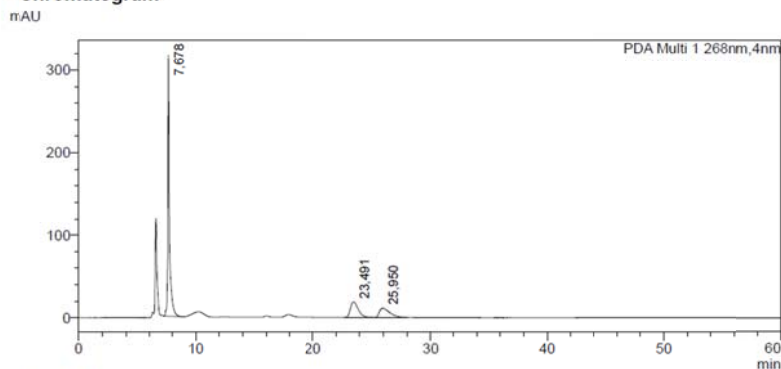
Peak#	Ret. Time	Area	Height	Conc.	Unit	Mark	Name
1	13.396	11083420	886153	0,000			
2	58.752	3801599	34633	0,000		M	
3	68.810	3805044	38825	0,000			
Total		18690063	959612				

2c (Chiralpak-ASH n heptane:iPrOH 99.5:0.5, 0.5 ml/min)

SHIMADZU LabSolutions 2c



<Chromatogram>

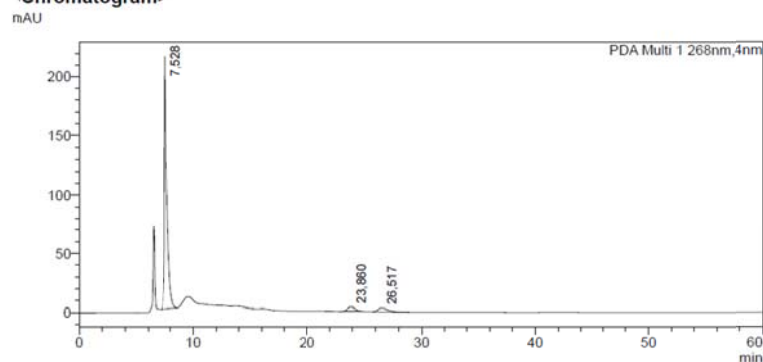


<Peak Table>

Peak#	Ret. Time	Area	Height	Conc.	Unit	Mark	Name
1	7.678	3015626	316830	0.000			
2	23.491	873991	18822	0.000			
3	25.950	681794	11126	0.000		V	
Total		4571411	346778				

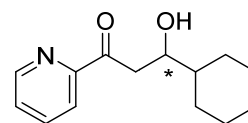
SHIMADZU LabSolutions 2c racemate

<Chromatogram>



Peak#	Ret. Time	Area	Height	Conc.	Unit	Mark	Name
1	7.528	3242814	214666	0.000			
2	23.860	178347	3963	0.000		M	
3	26.517	177341	3147	0.000			
Total		3598502	221775				

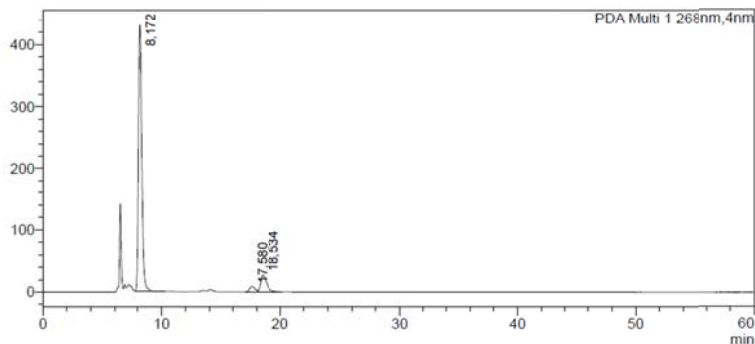
**2d** (Chiralpak-ASH n heptane:iPrOH 98:2, 0.5 ml/min)



SHIMADZU LabSolutions **2d**

<Chromatogram>

mAU



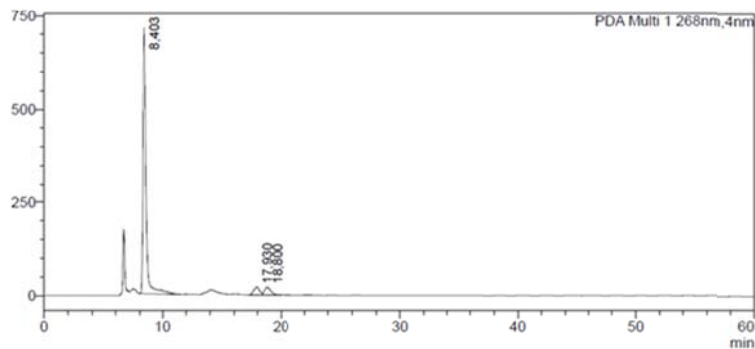
PDA Ch1 268nm

Peak#	Ret. Time	Area	Height	Conc.	Unit	Mark	Name
1	8.172	8460185	430814	0,000		S	
2	17.580	285888	9059	0,000			
3	18.534	995779	27175	0,000		V	
Total		9741852	467048				

SHIMADZU LabSolutions **2d racemate**

<Chromatogram>

mAU



<Peak Table>

PDA Ch1 268nm

Peak#	Ret. Time	Area	Height	Conc.	Unit	Mark	Name
1	8.403	14952181	711981	91,070		S	
2	17.930	733703	21444	4,469		M	
3	18.800	732399	20854	4,461		V M	
Total		16418283	754279				

## 8. Saturation Kinetics

The catalytic parameters were determined for LmrR\_M89X and LmrR\_M89X\_V15E using reverse-phase HPLC (rp\_HPLC), C18 column equipped with pre-column (*Phenomenex*, 4.6 mm internal diameter) with substrate **1a**, using caffeine as a standard. (Acetonitrile/water gradient, 65 min 0.5 ml/min). The catalytic solution was prepared as in standard catalysis, by combining  $\text{Cu}(\text{H}_2\text{O})_6(\text{NO}_3)_2$  (90  $\mu\text{M}$ , 9 % catalyst loading) with 1.25 equivalents of LmrR\_M89X/M89X\_V15E (112.5  $\mu\text{M}$ ) in a final volume of 435  $\mu\text{L}$  MOPS buffer (20 mM MOPS, 250mM NaCl, pH 7.0) and incubating together at 4 °C for one hour. The reaction was started by adding 15  $\mu\text{L}$  of a fresh stock solution of substrate **1a** in  $\text{CH}_3\text{CN}$  (final concentration in reaction mixture varied from 0.25 to 3 mM), sample was thoroughly mixed and immediately run on rp-HPLC. Over time (every 65 min) a sample was injected on the column and analyzed. The same experiment was performed without addition of protein and  $\text{Cu}(\text{H}_2\text{O})_6(\text{NO}_3)_2$ . For each used substrate concentration, the concentrations of the product were plotted against time and the initial rate of the reaction ( $v_0$ ) was determined from the linear part of the curve. The kinetic parameters were obtained by fitting the data to *Equation 1* using Origin software 8.5. The observed inequivalence of the cofactors in the MD simulations raises the possibility of cooperativity. The quality of the fit to the Hill equation, which applies to cooperative enzyme catalysis, is equal to that of the Michaelis-Menten analysis (Fig. S10). Yet, in absence of supporting experimental proof for cooperativity, the Michaelis-Menten analysis was preferred. For the fitting of the cooperativity, Hills equation (*Equation 2*) was applied using the same software.

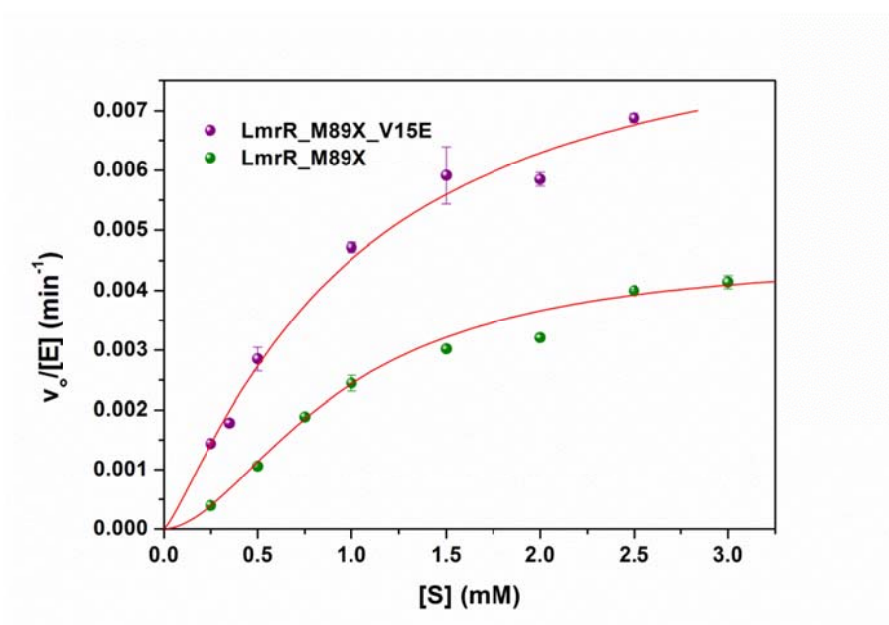
$$\frac{v_0}{[\text{E}]} = \frac{k_{\text{cat}}[\text{S}]}{K_{\text{M}} + [\text{S}]}$$

(Equation 1)

$$\frac{v_0}{[\text{E}]} = \frac{k_{\text{cat}}[\text{S}]^n}{(K_{0.5})^n + [\text{S}]^n}$$

(Equation 2)

a)



b)

<i>Catalyst</i>	$K_{0.5}$ (mM)	$k_{cat}$ (min <sup>-1</sup> )	n	<i>Fit</i> <i>R-Square</i>
LmrR_M89X_Cu(II)	0.93578±0.0779	0.0046±0.0003	1.790±0.147	0.994
LmrR_M89X_V15E_Cu(II)	0.97489±0.2986	0.0089±0.0013	1.217±0.157	0.993

**Figure S10** a) Kinetics of the hydration of **1a** catalyzed by LmrR\_M89X and LmrR\_M89X\_V15E. The red line represents the fit obtained using the Hill equation (Equation 2 above) b) Table with the catalytic parameters obtained using the Hill equation.

## 9. References

1. P. K. Madoori, H. Agustiandari, A. J. M. Driessen, and A.-M. W. H. Thunnissen, *EMBO J.*, 2009, **28**, 156.
2. Gaussian 09, Revision D.01, M. J. Frisch, G. W. Trucks, H. B. Schlegel, G. E. Scuseria, M. A. Robb, J. R. Cheeseman, G. Scalmani, V. Barone, B. Mennucci, G. A. Petersson, H. Nakatsuji, M. Caricato, X. Li, H. P. Hratchian, A. F. Izmaylov, J. Bloino, G. Zheng, J. L. Sonnenberg, M. Hada, M. Ehara, K. Toyota, R. Fukuda, J. Hasegawa, M. Ishida, T. Nakajima, Y. Honda, O. Kitao, H. Nakai, T. Vreven, J. A. Montgomery, Jr., J. E. Peralta, F. Ogliaro, M. Bearpark, J. J. Heyd, E. Brothers, K. N. Kudin, V. N. Staroverov, T. Keith, R. Kobayashi, J. Normand, K. Raghavachari, A. Rendell, J. C. Burant, S. S. Iyengar, J. Tomasi, M. Cossi, N. Rega, J. M. Millam, M. Klene, J. E. Knox, J. B. Cross, V. Bakken, C. Adamo, J. Jaramillo, R. Gomperts, R. E. Stratmann, O. Yazyev, A. J. Austin, R. Cammi, C. Pomelli, J. W. Ochterski, R. L. Martin, K. Morokuma, V. G. Zakrzewski, G. A. Voth, P. Salvador, J. J. Dannenberg, S. Dapprich, A. D. Daniels, O. Farkas, J. B. Foresman, J. V. Ortiz, J. Cioslowski, and D. J. Fox, Gaussian, Inc., Wallingford CT, 2013.
3. A. D. Becke, *J. Chem. Phys.*, 1993, **98**, 5648.
4. P. J. Stephens, F. J. Devlin, C. F. Chabalowski, and M. J. Frisch, *J. Phys. Chem.*, 1994, **98**, 11623.
5. G. A. Petersson, A. Bennett, T. G. Tensfeldt, M. A. Al-Laham, W. A. Shirley, and J. Mantzaris, *J. Chem. Phys.*, 1988, **89**, 2193.
6. G. A. Petersson and M. A. Al-Laham, *J. Chem. Phys.*, 1991, **94**, 6081.
7. R. L. Dunbrack, *Curr. Opin. Struct. Biol.*, 2002, **12**, 431.
8. E. F. Pettersen, T. D. Goddard, C. C. Huang, G. S. Couch, D. M. Greenblatt, E. C. Meng, and T. E. Ferrin, *J. Comput. Chem.*, 2004, **25**, 1605.
9. M. D. Eldridge, C. W. Murray, T. R. Auton, G. V. Paolini, and R. P. Mee, *J. Comput. Aided. Mol. Des.*, 1997, **11**, 425.
10. D.A. Case, J.T. Berryman, R.M. Betz, D.S. Cerutti, T.E. Cheatham, III, T.A. Darden, R.E. Duke, T.J. Giese, H. Gohlke, A.W. Goetz, N. Homeyer, S. Izadi, P. Janowski, J. Kaus, A. Kovalenko, T.S. Lee, S. LeGrand, P. Li, T. Luchko, R. Luo, B. Madej, K.M. Merz, G. Monard, P. Needham, H. Nguyen, H.T. Nguyen, I. Omelyan, A. Onufriev, D.R. Roe, A. Roitberg, R. Salomon-Ferrer, C.L. Simmerling, W. Smith, J. Swails, R.C. Walker, J. Wang, R.M. Wolf, X. Wu, D.M. York and P.A. Kollman (2015), AMBER 2015, University of California, San Francisco.
11. W. D. Cornell, P. Cieplak, C. I. Bayly, I. R. Gould, K. M. Merz, D. M. Ferguson, D. C. Spellmeyer, T. Fox, J. W. Caldwell, and P. A. Kollman, *J. Am. Chem. Soc.*, 1995, **117**, 5179.
12. W. L. Jorgensen, J. Chandrasekhar, J. D. Madura, R. W. Impey, and M. L. Klein, *J. Chem. Phys.*, 1983, **79**, 926.
13. C. I. Bayly, P. Cieplak, W. Cornell, and P. A. Kollman, *J. Phys. Chem.*, 1993, **97**, 10269.
14. J. M. Seminario, *Int. J. Quantum Chem.*, 1996, **60**, 1271.
15. J. Wang, R. M. Wolf, J. W. Caldwell, P. A. Kollman, and D. A. Case, *J. Comput. Chem.*, 2004, **25**, 1157.
16. U. Essmann, L. Perera, M. L. Berkowitz, T. Darden, H. Lee, and L. G. Pedersen, *J. Chem. Phys.*, 1995, **103**, 8577.
17. J.-P. Ryckaert, G. Ciccotti, and H. J. . Berendsen, *J. Comput. Phys.*, 1977, **23**,

- 327.
18. T. Schneider and E. Stoll, *Phys. Rev. B*, 1978, **17**, 1302.
  19. A. Brünger, C. L. Brooks, and M. Karplus, *Chem. Phys. Lett.*, 1984, **105**, 495.
  20. S. Duane, A. D. Kennedy, B. J. Pendleton, and D. Roweth, *Phys. Lett. B*, 1987, **195**, 216.
  21. P. Eastman and V. S. Pande, *Comput. Sci. Eng.*, 2015, **12**, 34.
  22. I. Drienovská, A. Rioz-Martínez, A. Draksharapu, and G. Roelfes, *Chem. Sci.*, 2015, **6**, 770.
  23. T. S. Young, I. Ahmad, J. A. Yin, and P. G. Schultz, *J. Mol. Biol.*, 2010, **395**, 361.
  24. J. Bos, A. García-Herraiz, and G. Roelfes, *Chem. Sci.*, 2013, **4**, 3578.